Journal of Electrical Engineering, Vol. 75, No. 3, 2024, pp. 214-223

sciendo

PAPERS

High-performance MTM inspired two-port MIMO antenna structure for 5G/IoT applications

Samia Hamdan[1], Ehab K. I. Hamad[2], Hesham A. Mohamed[3], Sherif A. Khaleel[4, *]

This study thoroughly investigates a two-port multiple-input multiple-output (MIMO) antenna system tailored for 5G operation at 28 GHz. The proposed antenna is patched on a Rogers (RT5880) substrate with a relative permittivity of 2.2 and total size of 20×12×0.508 mm^3. The mutual relationship between the radiating patches is refined using an H-shaped metamaterial structure to reduce the isolation to –55 dB. A MIMO configuration with attractive features is employed to reduce the envelope correlation coefficient (*ECC*) to about 0.00062 and the channel capacity loss (*CCL*) to about 0.006 bits/sec/Hz, while magnify the gain to about 9.39 dBi and the diversity gain (*DG*) to about 9.995. Additionally, it boasts a compact size with stable radiation pattern. The simulations of the MIMO antenna are executed using CST microwave studio, subsequently validated with Advanced Design System (ADS) for an equivalent circuit model, then measured using Vector Network Analyzer. Discrepancies between measured and simulated results were analyzed, with observed variations attributed to cable losses and manufacturing tolerances. Despite these challenges, a comprehensive comparison with prior research highlights the notable advantages of the proposed design, positioning it as a compelling solution for 5G applications.

Keywords: antenna, IoT, MIMO, high isolation, 5G, metamaterial

1 Introduction

Over the past decade, significant strides in wireless communication have led to the emergence of 5G technology, driven by the need to accommodate large user bases with high-speed data transfer. MIMO antennas offer multiple-user support, longer range and coverage, better connection dependability, higher data throughput, and improved spectral efficiency. This integration results in increased network performance, especially in demanding operating situations, faster and more reliable wireless communication, and effective spectrum usage. Reducing signal correlation between antenna parts is the main goal of MIMO antenna design, necessitating enhanced isolation and reduced mutual coupling for optimized radiation patterns and interference mitigation. The millimeter wave spectrum is being increasingly recognized as a viable option for the forthcoming 5G mobile network. In line with this, the FCC has designated a frequency range of 25 to 70 GHz specifically for 5G communications [1-5].

Recently, a dual-band 28/38 GHz MIMO antenna was developed by researchers [6, 7]. In [8], A four-port MIMO antenna, integrating a parasitic element, has been presented. Initially designed for 28 GHz applications, the antenna underwent adjustments such as slot etching and stub loading to enable dual-band operation at 28/38 GHz with a wide operational bandwidth and reduced return losses. Subsequently, a four-port MIMO setup was established by incorporating a parasitic element to reduce the mutual interference between the four antenna components. In [9], the paper introduced a compact eight-element MIMO antenna array with miniaturized loop elements, boasting a low profile and high isolation of –20 dB between elements without auxiliary isolation techniques. In [10], A low-profile two-port MIMO setup is proposed for 5G mm-wave applications at 28 GHz. Initially, a rectangular slot in the ground plane and circular cuts at the radiating patch's borders are used to create a single antenna element. This element is then modified into a two-element MIMO system with a decoupling slab between them. This enhances bandwidth to 2 GHz and attains a significant gain of 8.75 dB at 28.5 GHz, with a high level of isolation reached to –64 dB at 28 GHz. Simulated MIMO characteristics, including diversity gain (*DG*) and envelope correlation coefficient (*ECC*), meet the desired criteria, affirming the antenna's suitability for 5G communications. In [11], a novel MIMO antenna with two elements has been designed with focus on enhancing isolation characteristics. Through meticulous analysis, a dual-function decoupling mechanism was implemented, efficiently controlling, and suppressing the propagation of surface waves. This design incorporates an H-shaped for the

[1] Electronics & Comm. Dept., Luxor Higher Institute of Engineering & Technology, Luxor 85834, Egypt
[2] Electrical Engineering Department, Faculty of Engineering, Aswan University, Aswan 81542, Egypt
[3] Microstrip Circuits Department, Electronics Research Institute, Elnozha, Cairo 11843, Egypt
[4] Department of Electronics & Communications Engineering, College of Engineering and Technology, Arab Academy for Science, Technology and Maritime Transport (AASTMT), Aswan 81511, Egypt
* sherif.abdalla@aast.edu

https://doi.org/10.2478/jee-2024-0026, Print (till 2015) ISSN 1335-3632, On-line ISSN 1339-309X

isolation process using a defective ground structure (DGS). The resulting antenna achieves satisfactory suppression of coupling, compact planar dimensions, and a low profile. Utilizing only a single substrate layer makes the design cost-effective and easily scalable for larger MIMO configurations. In [12], a compact MIMO antenna array with high isolation is presented, leveraging metamaterial unit cells for enhanced isolation. With a gain of 10.2 dBi, it significantly reduces mutual coupling by –35 dB at 28 GHz. Evaluation via correlation and diversity gain coefficients validates its effectiveness, supported by experimental measurements demonstrating over –50 dB isolation at 28 GHz and an envelope correlation of approximately 0.0001. In [13], a 2-port MIMO substrate integrated waveguide (SIW) antenna operating at 28/38 GHz dual bands and boasting a peak gain of more than 5 dBi is shown. [14] explores a four-element MIMO/array antenna operating at 28/38 GHz in dual bands, obtaining a simulated peak gain of 9 dBi. Additionally, [15] presents a dual-band 28/38 GHz loop antenna with six ports, more than –25 dB isolation, and a simulated peak gain of more than 4.5 dBi.

This research proposes a two-element MIMO antenna for 5G applications that has high isolation performance. An MTM unit cell is suggested to enhance the isolation between the patches by –55 dB. The dimensions of Rogers 5880 substrate were 20×12×0.508 mm^3. The rest of the paper is structured as follows: The suggested antenna design is described in Section Two with the single and MIMO configurations, also introducing the MTM structure for isolation enhancement. Then, the MIMO antenna parameters such as the envelope correlation coefficient and diversity gain are introduced in Section Three. Finally, the conclusions are presented in the last section.

2 Antenna design and analysis

2.1 Single element antenna design

Firstly, a traditional microstrip patch antenna is designed on a Rogers 5880 substrate with a thickness of $h_c = 0.508$ mm, $\varepsilon_r = 2.2$ and loss tangent of 0.0009.

Schematic diagram of the proposed single element is presented in Fig. 1. As illustrated in Fig. 2, the suggested antenna is developed to resonate at 28 GHz. Table 1 contains tabulation of the antenna's optimal dimensions. The single port design is matched to a transmission line of 50 Ω characteristic impedance using an inset feed method using CST microwave studio. The ADS software is used for the validation process. As shown in Figs. 2(a, b), the findings from the CST microwave studio and the ADS circuit model are in good agreement. The values of the RLC equivalent circuit model of the antenna are listed in Tab. 1.

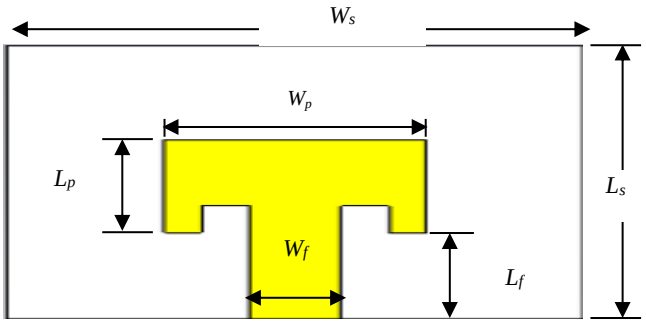

Fig. 1. Schematic diagram of a single element patch antenna

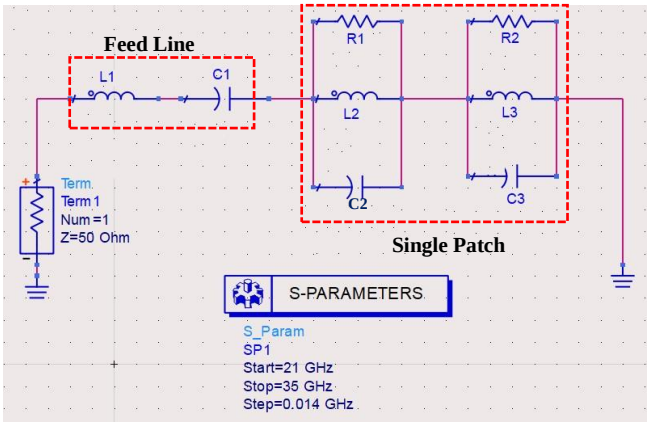

(a)

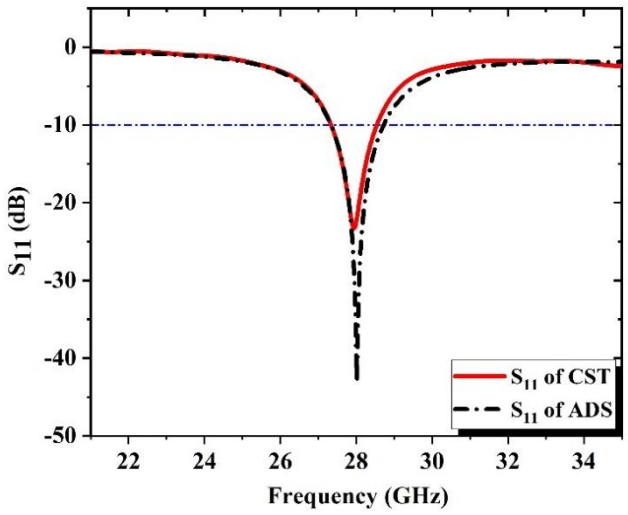

(b)

Fig. 2. (a) Equivalent circuit schematic (ADS) of the single patch antenna, and (b) the S_{11} of CST and ADS simulation

Table 1. Desired antenna parameters

Parameter	Value (mm)	Parameter	Value (mm)
W_s	9.4	L_s	10.3
W_p	4.24	L_p	3.83
W_f	1.565	L_f	3
RLC of Antenna using ADS model			
$L_1 = L_4$	11.6 pH	$C_1 = C_4$	1.8 pF
$L_2 = L_5$	15.1 pH	$C_2 = C_5$	5 pF
$L_3 = L_6$	20.2 pH	$C_3 = C_6$	1.9 pH
$R_1 = R_3$	50.2 Ω	$R_2 = R_4$	45.2 Ω
L_7	3.5 pH	C_7	0.2 pF
L_8	9.5 pH	C_8	0.8 pF
L_9	103.3 pH	C_9	1.53 pF

The 3D far-field pattern of the proposed antenna structure is illustrated in Fig. 3 with a gain value of 8.43 dBi.

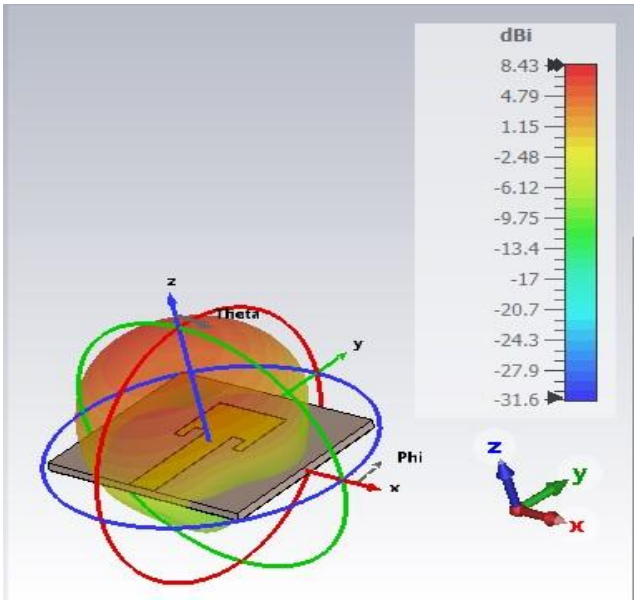

Fig. 3. The 3D far field of the proposed antenna design

2.2 Two-element MIMO antenna structures

A two-element MIMO configuration has been created using the suggested single-element antenna described in this paper. Figure 4 illustrates the MIMO antenna configurations namely, side-by-side, orthogonal, and face-to-face directions. The separated distance (d) is responsible for the coupling between the radiating elements. It must be consistent in all the configurations. The S-parameters of the proposed configuration are illustrated in Fig. 5. The S-parameters of the three proposed MIMO configurations listed in Fig. 5 reveal that S_{11} parameters are identical at 28 GHz resonance frequency, while the S_{21} (mutual coupling parameters) fluctuate according to the degree of coupling. Compared to the other designs that provide –22 dB and –25 dB mutual couplings for side-by-side and Orthogonal configurations, respectively, the face-to-face antenna configuration has a minimal isolation value of –33 dB over the whole bandwidth.

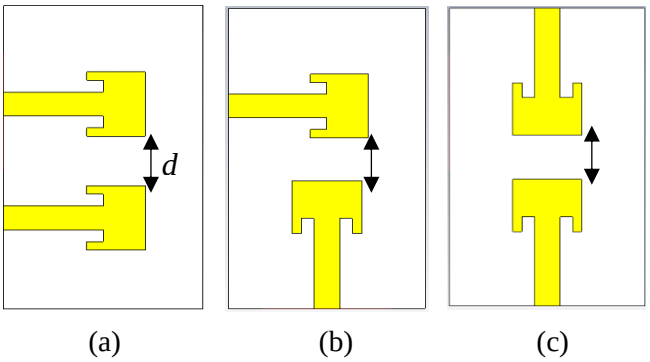

Fig. 4. MIMO configuration (a) side-by-side, (b) orthogonal, and (c) face-to-face

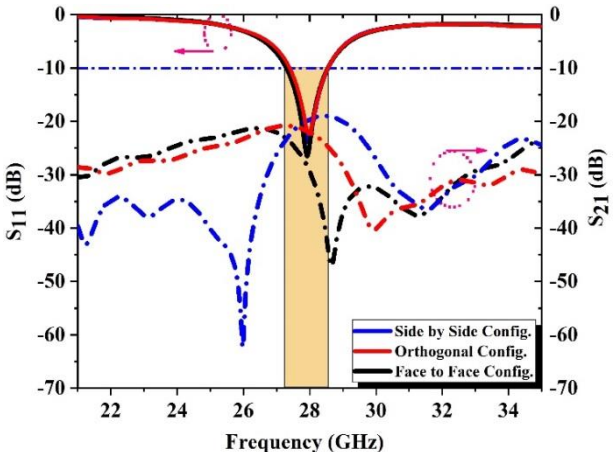

Fig. 5. S-parameters of the MIMO configurations

2.3 Decoupling MTM structure

The coupling problem between the two radiating conductors can be avoided by using an MTM resonator structure that is constructed by circular and rectangular unit cells as shown in Fig. 6. This proposed structure is said to be an MTM unit cell if its relative permittivity and/or permeability has a negative value throughout the resonance frequency as illustrated in Fig. 7(a). The MTM unit cell works as a band stop filter with a strong band rejection characteristic (S_{21}) between the radiating patches as indicated in the S-parameters curves that are depicted in Fig. 7(b). The equivalent circuit model of the MTM structure is carried out using ADS software as depicted in Fig. 7(c).

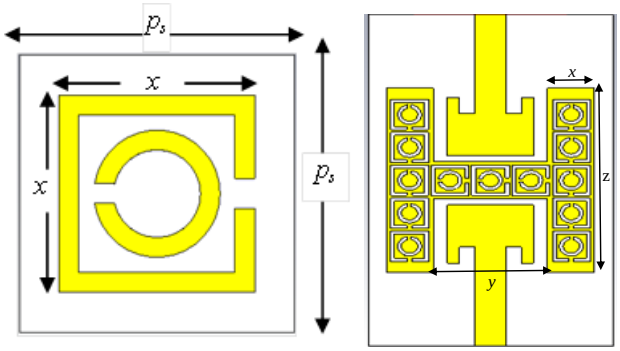

(a) (b)

Fig. 6. (a) MTM structure unit cell, and (b) the proposed MIMO antenna with an MTM unit cell

The S-parameters of the MTM structure in CST have good agreement with its values in ADS software with a good band rejection characteristic throughout the resonance frequency of 28 GHz. The integration of the MTM structure enhances the isolation between the radiating patches and reduces mutual coupling as depicted in Figs. 8(a, b). This figure revealed that S_{21} of the proposed MIMO antenna configuration (isolation coefficient) is reduced from –30 dB to –55 dB while the S_{11} is the same within the entire bandwidth. So, there is a notable decrease in the net interference between the two patches. The equivalent circuit model may be used to validate these findings throughout the ADS software which gives asymptotic results with the CST simulation. As shown in Fig. 8(c), the equivalent circuit model has two input ports with a 50 Ω input impedance that are divided by an H-shaped MTM RLC resonator.

The fabricated face-to-face MIMO antenna structure prototype is illustrated in Fig. 9 and the measured S-parameters are executed using (ZVA 67) network analyzer. The two components of the MIMO antenna are identical and symmetrically organized. During the tests, only one port receives stimulation, and the other port is terminated with a 50 Ω load. Figure 8 shows the proposed MIMO antenna's simulated and measured S-parameters. This figure demonstrates a close alignment between the measured S-parameters of the antenna and those simulated using ADS and CST software, although a slight frequency shift is observed due to the fabrication losses.

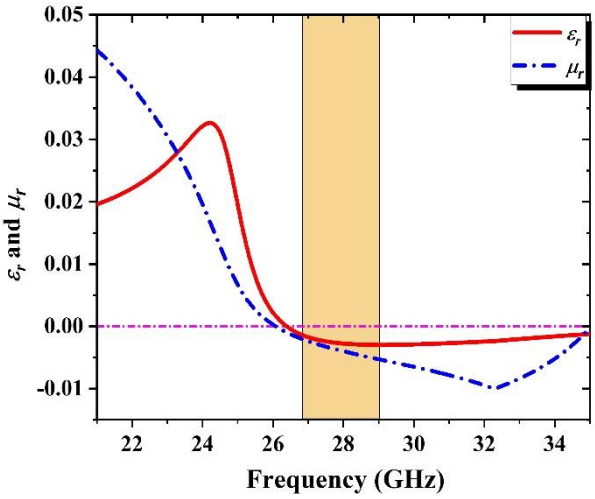

(a)

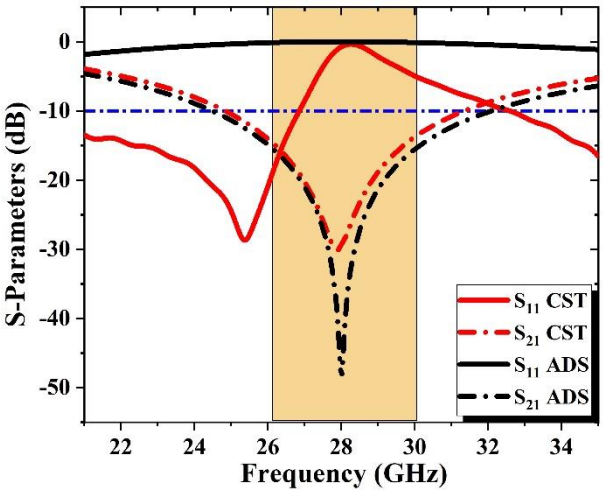

(b)

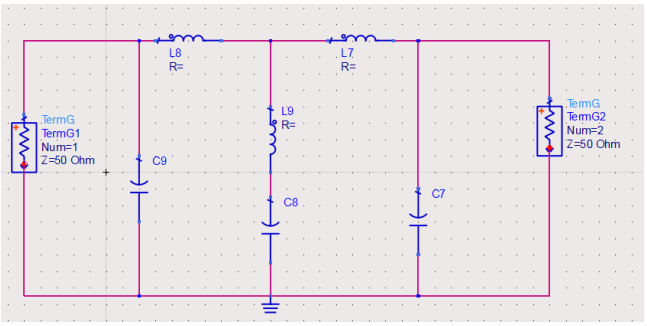

(c)

Fig. 7. The MTM unit cell parameters: (a) relative permittivity and permeability, (b) S-parameters of CST and ADS, and (c) the equivalent circuit model RLC

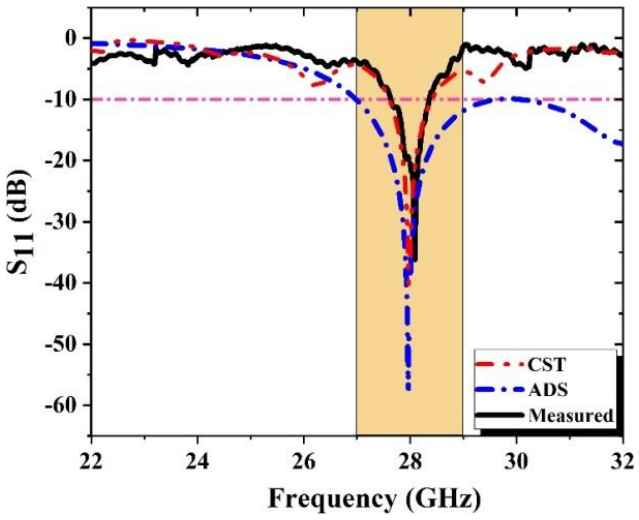

(a)

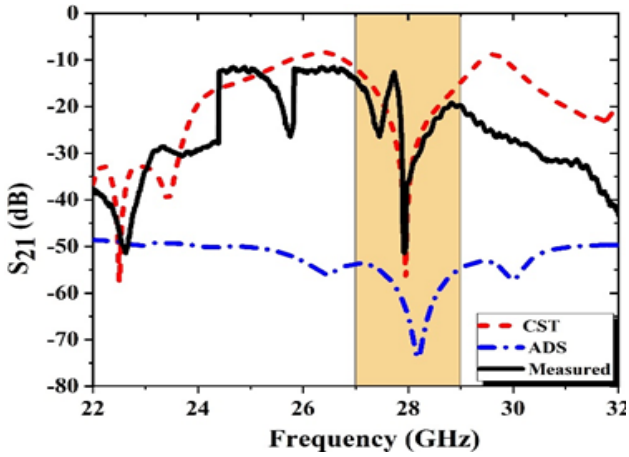

(b)

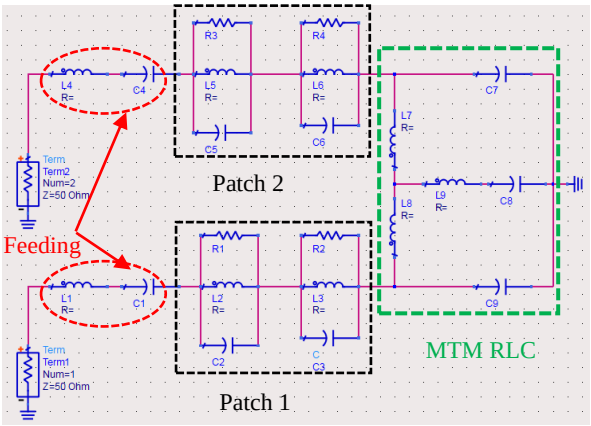

(c)

Fig. 8. MIMO antenna parameters (a, b) S-parameters, and (c) ADS equivalent circuit model with MTM resonator

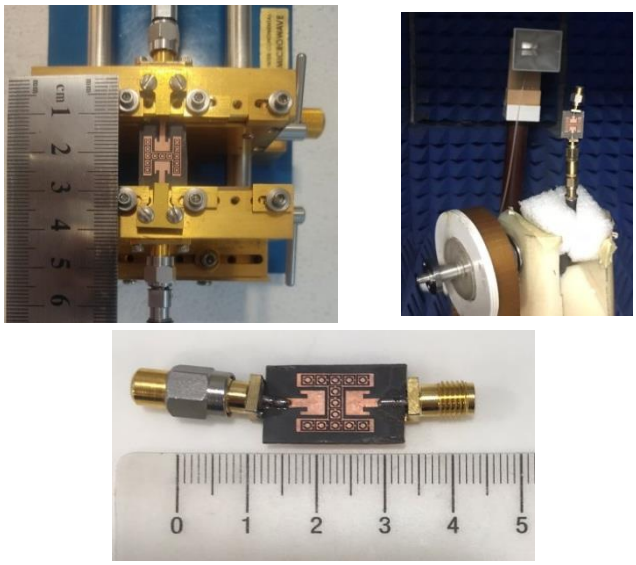

Fig. 9. Fabrication of the proposed MIMO antenna structure

Figure 10 shows the surface current distribution of the proposed MIMO antenna configuration. This figure demonstrates that in the absence of the H-shape MTM structure, there is considerable mutual coupling between the two radiating patches. Conversely, with the inclusion of the MTM unit cell, there is a marked reduction in mutual coupling and current density between the patches, this outcome ensures the S-parameters, which produce the same effects.

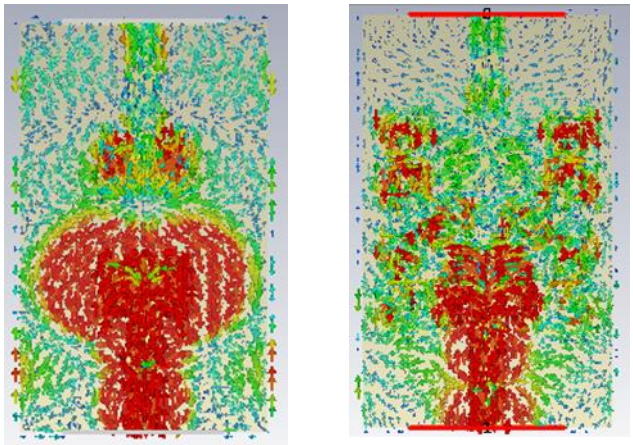

(a) (b)

Fig. 10. The current distribution of the MIMO antenna (a) without the MTM, and (b) with the MTM unit cell

The E-plane and H-plane radiation pattern (simulated and measured) at 28 GHz is shown in Fig. 11 when the antenna is activated at port 1 and the other port is terminated by a 50 Ω load. The proposed values of the electric and magnetic fields have a consistent trend between the simulated and measured results with a small deviation because of the measurements setup. Figure 12 also presents the proposed antenna's 3D radiation pattern. This figure illustrated that the gain of the antenna for the MIMO structure with the MTM structure's presence increased from 8.43 dBi to 9.39 dBi for the single one.

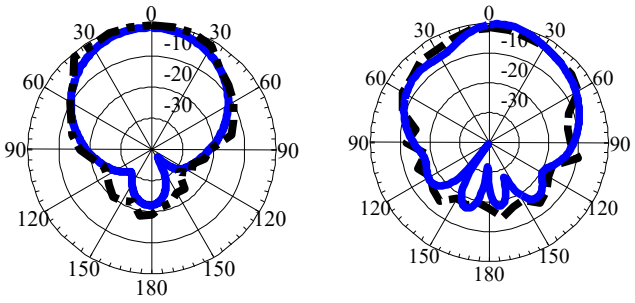

(a) (b)

Fig. 11. Measured and simulated far-field radiation of MIMO antenna (a) E-plane, and (b) H-plane: simulated (solid line) – measured (dashed line)

3 Studying MIMO antenna parameters

Here, we discuss the MIMO parameters which are considered very crucial in the MIMO mechanism. The diversity gain, channel capacity loss and envelope correlation coefficient are evaluated and discussed [16, 17]. The envelope correlation coefficient is a metric used to assess the correlation between patches within a chosen MIMO configuration. Reduced *ECC* values signify enhanced MIMO performance. *ECC* can be derived through various methods, one of which involves extraction from S-Parameters, as outlined in the following equation [18].

The envelope correlation coefficient is expressed as

$$ECC = \frac{|S_{11}^{*}S_{12} + S_{21}^{*}S_{22}|^2}{\left(1-(|S_{11}|^2+|S_{21}|^2)\right)\left(1-(|S_{22}|^2+|S_{12}|^2)\right)}, \quad (1)$$

where S_{11}^{*} and S_{21}^{*} are the conjugates of $S_{11}$and S_{21}, respectively. The acceptable limit of the *ECC* should be lower than 0.5.

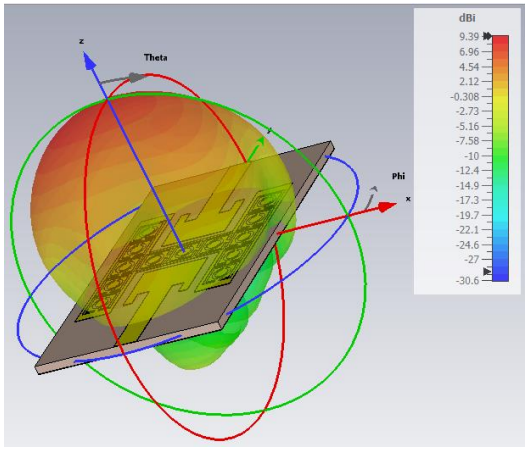

Fig. 12. 3D radiation pattern of the proposed MIMO antenna with the presence of an MTM unit cell

ECC is calculated and presented in Fig. 13(a). In this figure, the value of *ECC* is calculated in the presence and absence of the H-shape MT structure. Its value in the presence of the MTM is 0.00062 while in the absence of the MTM unit cell is 0.0211. The good MIMO antenna performance is achieved by its low *ECC* value. *ECC* of the MIMO antenna can be used to determine the diversity gain *DG* using the following relation [19].

$$DG = 10\sqrt{1-(ECC)^2} \quad (2)$$

In the optimal scenario where *ECC*=0, an ideal diversity gain of 10 dB is anticipated. Consequently, in practical contexts, achieving a minimal *ECC* value is crucial to approach a *DG* value nearing 10 dB. For our proposed MIMO configuration illustrated in Fig. 13 (b), the diversity gain values are calculated at 9.71 dB and 9.995 dB with and without the inclusion of the MTM unit cell, respectively. The channel capacity loss is a crucial metric in MIMO antenna systems, quanti-fying the degradation in channel capacity due to correlations between antenna elements. A well-designed MIMO setup aims to keep the *CCL* below 0.5 (bits/s/Hz) across the operational frequency range.

Equation (3) provides the formal representation for computing *CCL*, as defined in prior research [20]

$$CCL = -\log_2(\varphi^R), \tag{3}$$

$$\varphi^R = \begin{bmatrix} \rho_{11} & \rho_{12} \\ \rho_{21} & \rho_{22} \end{bmatrix}, \tag{4}$$

$$\rho_{ii} = \left(1 - \left(|S_{ii}|^2 + |S_{ij}|^2\right)\right), \tag{5}$$

$$\rho_{ij} = -\left(S_{ii}^* S_{ij} + S_{ij}^* S_{jj}\right), \tag{6}$$

where φ^R represents the receiving antenna's correlation matrix. Figure 13(c) shows a comparison of the *CCL* curves with and without the H-shaped metamaterial unit cell introduced. It has a value of 0.006 and 0.822, respectively. The mean effective gain (*MEG*) quantifies the average power received by the antenna in a fading environment relative to the combined power received from two isotropic antennas. It is calculated using the following formula [21]:

$$MEG = 0.5\left(1 - \sum_{j=1}^{M} |S_{ij}|^2\right), \tag{7}$$

where *M* represents the total number of MIMO patches. The *MEG* value should be more than −12 dB and less than −3 dB. The value of *MEG* is within an acceptable range both with and without the MTM unit cell, as Fig. 14(a) shows. The total active reflection coefficient (*TARC*) of the MIMO antenna characterizes its radiation performance, as described in [18]. It can be computed using the following relationship and illustrated in Figure 14(b):

$$TARC = \sqrt{\frac{|S_{11} + S_{12}e^{j\theta}|^2 + |S_{21} + S_{22}e^{j\theta}|^2}{2}}. \tag{8}$$

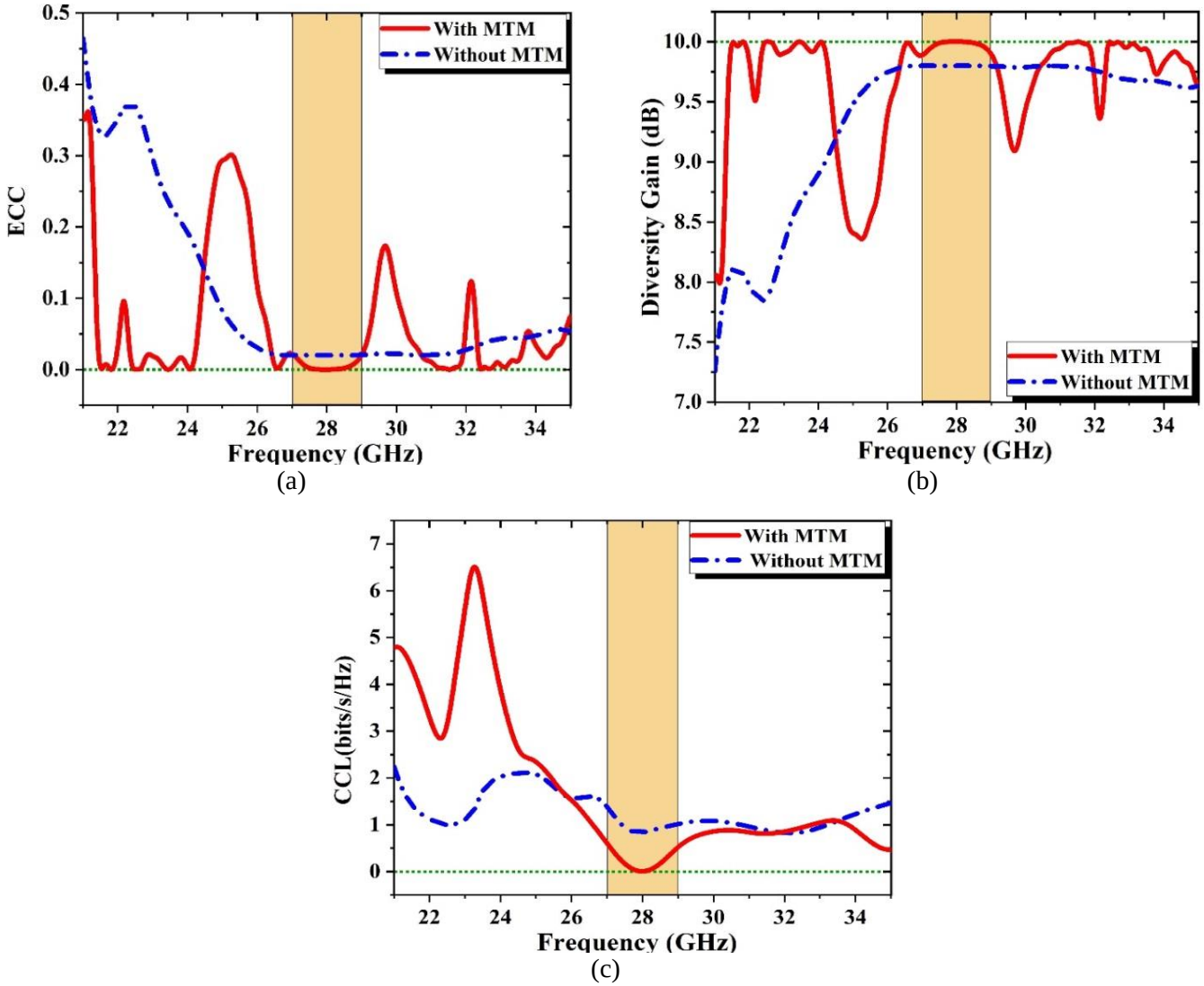

Fig. 13. (a) *ECC*, (b) *DG*, and (c) *CCL* of the MIMO antenna design

In this section, a comparative evaluation is conducted between the proposed optimized MIMO design and previously reported designs for the mm-wave antennas. The comparison assesses performance metrics such as gain, antenna element, dimensions, and resonance frequency. Furthermore, the parameters of MIMO including *CCL*, *DG*, and *ECC* are compiled in Table 2 for comprehensive analysis.

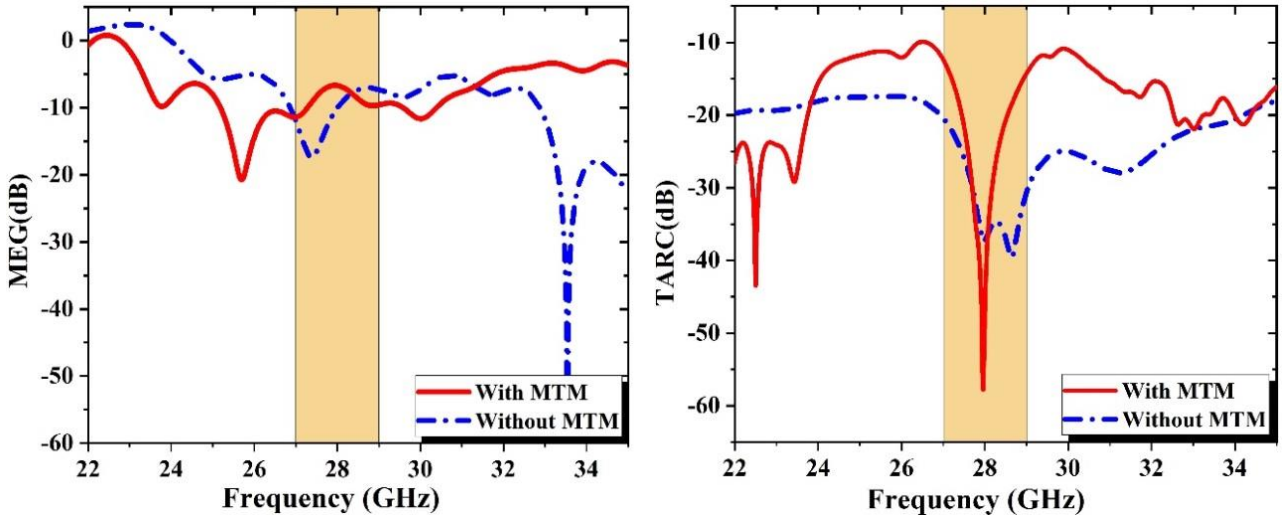

(a) (b)

Fig. 14. (a) *MEG* and (b) *TARC* parameters of the MIMO antenna.

Table 2. Parameters of MIMO including *CCL*, *DG*, and *ECC*

Ref.	Freq. (GHz)	Size (mm^3)	No. of elements	Decoupling method	Isolation (dB)	Gain (dBi)	*ECC*/*DG* (dB)	*CCL* (bits/sec/Hz)
[21]	28	30 × 15 × 0.25	2	DGS	–35.8	5.42	0.005/9.99	< 0.1
[22]	28	30 × 35 × 0.76	4	DGS	–17	8.3	0.01/9.96	< 0.4
[23]	28	28.3 × 28.3 × 0.787	4	MTM + DGS	–40	11	0.00001/9.999	<0.4
[24]	18/28	13× 6.2 × 0.72	2	DGS	–20	5.4	< 0.22/ 9.6	< 0.25
[25]	28/38	26 × 14.5 × 0.508	2	MTM + DGS	–39/–38	5.2/5.5	0.0001/9.99	0.05
[26]	28	9.4 × 17 × 0.508	2	MTM and CMA	–27	8.31	0.001/10	0.0016
[27]	30/38	27 × 27 × 1.52	4	-	–42	8.4	0.001/9.99	0.01
[28]	28/38	80 × 80 × 1.57	4	-	–20	12	0.0014/-	-
[29]	28	31.89×37.59×0.508	4	DGS	–18	5.76	0.004/9.95	0.4
Proposed	28	20 × 12 x 0.508	2	MTM	–55	9.39	0.00062/9.995	0.006

4 Conclusion

This research paper demonstrated a high performance two-port MIMO antenna configuration for 5G mm-wave and IoT applications. The proposed MIMO has a very compact size of 20×12×0.508 mm^3 and it can be easily fabricated with a resonance frequency of 28 GHz. Incorporating an H-shaped MTM structure, mutual coupling between radiating patches is significantly reduced from –30 dB to –55 dB. The proposed MIMO antenna, enhanced with an H-shaped MTM structure, achieved a gain of 9.39 dBi. The overall results of the proposed MIMO antenna design are achieved by CST microwave studio and the results are verified by the equivalent circuit model using ADS. The fabrication process is distinguished and has good agreement with the simulated ones. The proposed design ensures reliable performance. Meeting MIMO performance parameters such as *ECC*=0.00062, *DG*=9.995, and *CCL*=0.006 within acceptable limits underscores the antenna's suitability for 5G mm-wave and cellular devices.

References

[1] D. Loghin, S. Cai, G. Chen, T. T. A. Dinh, F. Fan, Q. Lin, J. Ng B. C. Ooi, X. Sun, W. Wang, X. Xiao, Y. Yang, M. Zhang, and Z. Zhang "The disruptions of 5G on Data-Driven technologies and applications," *IEEE Transactions on Knowledge and Data Engineering*, vol. 32, no. 6, pp. 1179–1198, Jun. 2020, doi: 10.1109/tkde.2020.2967670.

[2] N. Al-Falahy and O. Alani, "Millimetre wave frequency band as a candidate spectrum for 5G network architecture: A survey," *Physical Communication*, vol. 32, pp. 120–144, Feb. 2019, doi: 10.1016/j.phycom.2018.11.003.

[3] B. Beiranvand, A. K. Iyer, and R. Mirzavand, "Cost-Effective design of a reflectarray antenna for 5G and Millimeter-Wave applications utilizing 3-D-Printed components," *IEEE Antennas and Wireless Propagation Letters*, vol. 23, no. 3, pp. 925–929, Mar. 2024, doi: 10.1109/lawp.2023.3338511.

[4] W. a. E. Ali, H. A. Mohamed, A. A. Ibrahim, and M. Z. M. Hamdalla, "Gain improvement of tunable band-notched UWB antenna using metamaterial lens for high speed wireless communications," *Microsystem Technologies*, vol. 25, no. 11, pp. 4111–4117, Jan. 2019, doi: 10.1007/s00542-018-04285-z.

[5] T. G. Abouelnaga, E. K. I. Hamad, S. A. Khaleel, and B. Beiranvand, "Defining breast tumor location using a Four-Element wearable circular UWB MIMO antenna array," *Applied Sciences*, vol. 13, no. 14, p. 8067, Jul. 2023, doi: 10.3390/app13148067.

[6] W. a. E. Ali, S. Das, H. Medkour, and S. Lakrit, "Planar Dual-band 27/39 GHz Millimeter-wave MIMO Antenna for 5G Applications," *Microsystem Technologies*, vol. 27, no. 1, pp. 283–292, Jul. 2020, doi: 10.1007/s00542-020-04951-1.

[7] F. Alnemr, M. F. Ahmed, and A. A. Shaalan, "A compact 28/38 GHz MIMO circularly polarized antenna for 5 G applications," *Journal of Infrared, Millimeter, and Terahertz Waves*, vol. 42, no. 3, pp. 338–355, Feb. 2021, doi: 10.1007/s10762-021-00770-1.

[8] M. Hussain, W.A. Awan, E. M. Ali, M.S.Alzaidi,., Alsharef, D.H. ElKamchouchi, A.Alzahrani, and M.Fathy "Isolation improvement of parasitic Element-Loaded Dual-Band MIMO antenna for MM-Wave applications," *Micromachines*, vol. 13, no. 11, p. 1918, Nov. 2022, doi: 10.3390/mi13111918.

[9] R. Li, Z. Mo, H. Sun, X. Sun, and G. Du, "A Low-Profile and high-isolated MIMO antenna for 5G mobile terminal," *Micromachines*, vol. 11, no. 4, p. 360, Mar. 2020, doi: 10.3390/mi11040360.

[10] I. U. Din, S. Ullah, N. Mufti, R. Ullah, B. Kamal, and R. Ullah, "Metamaterial-based highly isolated MIMO antenna system for 5G smartphone application," *International Journal of Communication Systems*, vol. 36, no. 3, Nov. 2022, doi: 10.1002/dac.5392

[11] Z. Yang, J. Xiao, and Q. Ye, "Enhancing MIMO antenna isolation characteristic by manipulating the propagation of surface wave," *IEEE Access*, vol. 8, pp. 115572–115581, Jan. 2020, doi: 10.1109/access.2020.3004467.

[12] S. Hamdan, H. A. Mohamed, and E. K. H.. Hamad, "Design of High Isolation Two-Port MIMO Two-element Array Antenna Using Square Spilt-Ring Resonators for 5G Applications," *Int. J. Micro. Opt. Tech,* Vol. 17, No. 4, pp. 339-346, July 2022.

[13] P. Liu, X. Zhu, Y. Zhang, X. Wang, C. Yang, and Z. H. Jiang, "Patch antenna loaded with paired shorting pins and H-Shaped slot for 28/38 GHz Dual-Band MIMO applications," *IEEE Access*, vol. 8, pp. 23705–23712, Jan. 2020, doi: 10.1109/access.2020.2964721.

[14] A. E. Farahat and K. F. A. Hussein, "Dual-band (28/38 GHz) MIMO Antenna System for 5G Mobile Communications with Efficient DoA Estimation Algorithm in Noisy Channels," *Applied Computational Electromagnetics Society Journal*, vol. 36, no. 3, pp. 282–294, Apr. 2021, doi: 10.47037/2020.aces.j.360308.

[15] H. Marzouk, M. Ahmed, and A. Shaalan, "A novel dual-band 28/38 GHz AFSL MIMO antenna for 5G smartphone applications," in *Journal of Physics: Conference Series*, 2020, vol. 1447, no. 1, p. 012025: IOP Publishing.

[16] S. A. Khaleel, E. K. I. Hamad, and M. B. Saleh, "High-performance tri-band graphene plasmonic microstrip patch antenna using superstrate double-face metamaterial for THz communications," *Journal of Electrical Engineering*, vol. 73, no. 4, pp. 226–236, Aug. 2022, doi: 10.2478/jee-2022-0031.

[17] S. A. Khaleel, E. K. I. Hamad, N. O. Parchin, and M. A. Saleh, "MTM-Inspired Graphene-Based THZ MIMO antenna configurations using characteristic mode analysis for 6G/IoT applications," *Electronics*, vol. 11, no. 14, p. 2152, Jul. 2022, doi: 10.3390/electronics11142152.

[18] G. Saxena, Y. K. Awasthi, and P. Jain, "Design of metasurface absorber for low RCS and high isolation MIMO antenna for radio location & navigation," *AEU - International Journal of Electronics and Communications*, vol. 133, p. 153680, May 2021, doi: 10.1016/j.aeue.2021.153680.

[19] I. S. Naqvi, N. Hussain, A. Iqbal, M. Rahman, M. Forsat, S.S. Mirjavadi, and Y. Amin "Integrated LTE and Millimeter-Wave 5G MIMO antenna system for 4G/5G wireless terminals," *Sensors*, vol. 20, no. 14, p. 3926, Jul. 2020, doi: 10.3390/s20143926.

[20] N. Hussain, M.-J. Jeong, A. Abbas, and N. Kim, "Metasurface-Based Single-Layer wideband circularly polarized MIMO antenna for 5G Millimeter-Wave systems," *IEEE Access*, vol. 8, pp. 130293–130304, Jan. 2020, doi: 10.1109/access.2020.3009380.

[21] N. Hussain, W. A. Awan, W. a. E. Ali, S. I. Naqvi, A. Zaidi, and T. T. Le, "Compact wideband patch antenna and its MIMO configuration for 28 GHz applications," *AEU - International Journal of Electronics and Communications*, vol. 132, p. 153612, Apr. 2021, doi: 10.1016/j.aeue.2021.153612.

[22] M. Khalid, I. Naqvi, S., Hussain, N., Rahman, M., Fawad, Mirjavadi, S.S., Khan, M.J. and Amin, Y. "4-Port MIMO Antenna with Defected Ground Structure for 5G Millimeter Wave Applications," *Electronics*, vol. 9, no. 1, p. 71, Jan. 2020, doi: 10.3390/electronics9010071.

[23] S. Ghosh, G. S. Baghel, and M. V. Swati, "Design of a highly-isolated, high-gain, compact 4-port MIMO antenna loaded with CSRR and DGS for millimeter wave 5G communications," *AEU - International Journal of Electronics and Communications*, vol. 169, p. 154721, Sep. 2023, doi: 10.1016/j.aeue.2023.154721.

[24] B. G. P. Shariff, T. Ali, P. R. Mane, P. Kumar, and S. Pathan, "Compact wideband two-element millimeter wave MIMO antenna with CMT based modified T-shaped decoupling structure for mobile applications with estimated link budget in urban scenario," *AEU - International Journal of Electronics and Communications*, p. 155209, Feb. 2024, doi: 10.1016/j.aeue.2024.155209.

[25] B. a. F. Esmail and S. Koziel, "High isolation metamaterial-based dual-band MIMO antenna for 5G millimeter-wave applications," *AEU - International Journal of Electronics and Communications*, vol. 158, p. 154470, Jan. 2023, doi: 10.1016/j.aeue.2022.154470.

[26] A. Abdelaziz and E. K. I. Hamad, "Isolation enhancement of 5G multiple-input multiple-output microstrip patch antenna using metamaterials and the theory of characteristic modes," *International Journal of Rf and Microwave Computer-aided Engineering*, vol. 30, no. 11, Sep. 2020, doi: 10.1002/mmce.22416.

[27] S. A.Hussain, Taher, F., Alzaidi, M.S., Hussain, I., Ghoniem, R.M., Fathy, M. and Lalbakhsh, A.., "Wideband, High-Gain, and Compact Four-Port MIMO Antenna for Future 5G Devices Operating over Ka-Band Spectrum," *Applied Sciences*, vol. 13, no. 7, p. 4380, Mar. 2023, doi: 10.3390/app13074380.

[28] D.A .Sehrai, M. Abdullah, A. Altaf, SH . Kiani, F. Muhammad, M. Tufail, M. Irfan, A. Glowacz, and S. Rahman "A novel high gain wideband MIMO antenna for 5G millimeter wave applications," *Electronics*, vol. 9, no. 6, p. 1031, Jun. 2020, doi: 10.3390/electronics9061031.

[29] N. E. H. Nasri, M. E. Ghzaoui, S. Das, T. Islam, W. a. E. Ali, and M. Fattah, "A novel arc-shaped four-port wideband (21.8–29.1 GHz) MIMO antenna with improved characteristics for 5G NR networks," *International Journal of Communication Systems*, Feb. 2024, doi: 10.1002/dac.5746.

Samia Hamdan, she received the B.Sc. degree in electronics & communication engineering from Luxor Higher Institute of Engineering & Technology, Egypt in 2017. She is working now as a teaching/research Assistant at Luxor Higher Institute of Engineering & Technology. Her current research interests include antenna design, metamaterials, and 5G communications.

Ehab K. I. Hamad received the B.Sc. and M.Sc. degrees in electrical engineering from Assiut University, Egypt in 1994 and 1999, respectively and the Ph.D. degree in electrical engineering from Magdeburg University, Germany in 2006. From 1996 to 2001 he was a teaching/research assistant with the Aswan Faculty of Engineering, SVU, Egypt. From July 2001 to December 2006, he was a research assistant with the Chair of Microwave and Communication Engineering, University Magdeburg. From July 2010 to April 2011, he was with the School of Computing and Engineering, University of Huddersfield, U.K. as a postdoctoral research assistant. He is currently full professor for antenna engineering with the Aswan University, Aswan, Egypt. He works as external peer reviewer for the National Authority for Quality Assurance and Accreditation of Education (NAQAAE). His current research interests include microstrip antennas, mm-wave antennas, RIS, 5G/6G, metamaterials. He is a reviewer of many journals including IEEE Trans. Antennas and Propagation, IET Microwaves, Antennas, and Propagations, Electronics Letters, Radioengineering, PIERs, Journal of Electrical Engineering, Journal of Recent Advances in Electrical & Electronic Engineering, and Optical Microwave Technology Letters as well as many international conferences including EuCAP, National Radio Sciences, and Asia-Pacific Microwave Conference and some others on Easy Chair and EDAS.

Hesham A. Mohamed received his B.Sc. degree in electronics and communication engineering from the University of Menoufia in 2003 and received his M.Sc. and Ph.D. degree from Ain Shams University in 2009 and 2014, respectively. He is currently associate researcher at Electronics Research Institute (ERI), Giza, Egypt and a member of the IEEE (Institute of Electrical and Electronic Engineers). His research interests on microwave circuit designs, planar antenna systems, radar absorbing materials, energy harvesting and wireless power transfer, smart antennas, microstrip antennas, microwave filters, metamaterials, and MIMO antennas and its applications in wireless communications. He is a reviewer at the International Journal as following, IEEE Microwave and Wireless Components Letters, IEEE ACCESS, Microwave and Optical Technology Letters, and International Journal of Circuit Theory and Applications.

Sherif A. Khaleel received the B.E. and MSc degree in electronic and communication engineering from Arab Academy for Science, Technology and Maritime Transport (AASTMT), Egypt in 2012 and 2017. He received his Ph.D. degree in electrical engineering from Aswan University in the design a graphene microstrip patch antenna in the THz band for the 6G communications at the Faculty of Engineering, Aswan University, Aswan, Egypt in 2023. Now he works as assistant professor at the College of Engineering and Technology, Department of Electronics, and Communication, AASTMT, Aswan- Egypt. His current research interests include antenna design, metamaterials, 6G communications, THz materials. RIS in wireless communications, Breast cancer detection using microwave imaging, and mm-wave antennas in 5G communications. He is a reviewer of many journals including IEEE Access, Radio engineering, PIERs, The Journal of Electrical Engineering, and Optical and Quantum Electronics.

Received 16 March 2024